Surface Science 630 (2014) 101–108

Contents lists available at ScienceDirect

Surface Science

journal homepage: www.elsevier.com/locate/susc

Electrochemical, HR-XPS and SERS study of the self-assembly of biphenyl 4,4′-dithiol on Au(111) from solution phase

E.M. Euti [a], P. Vélez Romero [a,b], O. Linarez Pérez [a], G. Ruano [c,d], E.M. Patrito [a], G. Zampieri [c,d,*], E.P.M. Leiva [b], V.A. Macagno [a], F.P. Cometto [a,**]

[a] Departamento de Fisicoquímica, Instituto de Investigaciones Fisicoquímica de Córdoba (INFIQC), Facultad de Ciencias Químicas, Universidad Nacional de Córdoba, Córdoba, Argentina
[b] Departamento de Matemática y Física, Instituto de Investigaciones Fisicoquímica de Córdoba (INFIQC), Facultad de Ciencias Químicas, Universidad Nacional de Córdoba, Córdoba, Argentina
[c] Centro Atómico Bariloche, Comisión Nacional de Energía Atómica, Bariloche, Argentina
[d] Instituto Balseiro, Universidad Nacional de Cuyo, Bariloche, Argentina

ARTICLE INFO

Article history:
Received 29 April 2014
Accepted 14 July 2014
Available online 22 July 2014

Keywords:
Self-assembled monolayers
Dithiols
Electrochemistry
XPS
SERS

ABSTRACT

We report a comparative study of 4,4′-biphenyldithiol adlayers grown on Au(111) substrates in solution phase by different methods. Layers prepared by immersion in solutions of ethanol and n-hexane, with and without the use of a disulfide reducing agent (tris-carboxyethyl phosphine, TCEP), were characterized by electroreductive desorption, impedance spectroscopy, redox activity, high-resolution photoemission spectroscopy, and surface-enhanced Raman spectroscopy. It is shown that the simple immersion in an ethanolic solution leads to the formation of, at least, a bilayer with a high number of S – S bonds. The use of n-hexane as solvent produces a drastic reduction of these undesired bonds, and a similar result is obtained if the substrates prepared in the ethanolic solution are then washed with TCEP. The best results were obtained when the reducing agent was added into the ethanol solution, in which case all the characterizations were coincident in the formation of a single layer of standing-up molecules free of S – S bonds. The charge of the desorption peak and the relative intensity of the S2p and Au4f photoemission peaks both indicate a surface coverage $\theta \approx 0.2$. In the case of multilayers formed by immersion in pure ethanolic solutions, the Raman experiments indicate that intralayer S – S bonds are not formed, and hence that all the S – S bonds are of the interlayer type.

1. Introduction

Self-assembled monolayers (SAMs) on solid surfaces are widely studied due to their potential applications [1,2]. A SAM is built up of molecules with three distinguishable parts: a head-group bound to the surface, a spacer group, and a terminal group that confers a new chemical identity to the modified surface. The special case of SAMs made of dithiol (DT) molecules is particularly important for applications in nanotechnology and molecular electronics [3]. DT molecules may be adsorbed in a standing-up (SU, mono-coordinated) [4–7] or a lying-down (LD, bi-coordinated) [8–11] configuration depending on the preparation method and surface coverage. For example, Haiss et al. [12] have shown by means of photoelectron spectroscopy that both S atoms of the 1,5-pentanedithiol molecule are bound to the gold surface at short immersion times while only one S atom remains bound to the surface for long immersion times. Pasquali et al. [13] studied the adsorption of 1,4-benzenedimethanethiol (BMDT) from vapor phase under controlled conditions in vacuum by different spectroscopic techniques. They deduced that, at low exposures the BMDT molecules initially adsorb in a bi-coordinated configuration and then, as more molecules stick to the surface, they adopt an upright mono-coordinated configuration preserving their –SH groups on the vacuum side. The synthesis of –SH-terminated surfaces is of great interest, because as one thiol group serves to bind the molecules to the surface the other can act as nucleation centers for the connection to other functional units [14–19].

A problem that arises in the preparation of DT SAMs is the formation of S – S bonds. The occurrence of these bonds impairs the SAM properties because: i) they provide interlayer links for the growth of multilayers, and ii) the formation of bonds between neighboring molecules in the top layer cancels –SH terminal groups. The strategies to deal with these bonds are essentially two: to avoid the oxidative conditions needed for the formation of the bonds, or to use disulfide reducing agents to either prevent or remove the bonds. Esaulov et al. [20–22] have reported the successful preparation of SAMs of alkane and aromatic DTs using n-hexane N_2 saturated solutions in the absence of light. On the other side, Lundgren et al. [23] reported that gold nanoparticles

* Correspondence to: G. Zampieri, Centro Atómico Bariloche, Comisión Nacional de Energía Atómica, Instituto Balseiro, Universidad Nacional de Cuyo, Bariloche, Argentina. Tel.: +54 294 4445229.
** Correspondence to: F.P. Cometto, INFIQC, Departamento de Fisicoquímica, Fac. Ciencias Químicas, Univ. Nacional de Córdoba, 5000 Córdoba, Argentina. Tel.: +54 351 5353866.
E-mail addresses: zamp@cab.cnea.gov.ar (G. Zampieri), fcometto@fcq.unc.edu.ar (F.P. Cometto).

http://dx.doi.org/10.1016/j.susc.2014.07.021
0039-6028/

bound more efficiently on a octanedithiol monolayer after the layer was reactivated with a reducing agent (dithiothreitol, DTT).

SAMs that contain molecules with conjugated spacer groups, such as aromatic molecules, are attractive because their conducting character may become useful for future nanoelectronic devices. Biphenyl-derived molecules have been considered as potential constituents in molecular devices due to the extended delocalization of π-electrons [24,25]. The adsorption 1,4-benzenedimethanethiol has been studied from both vapor phase deposition in vacuum [13,26,27] and from deposition in solution phase [28–30]. Rifai et al. have reported an electrochemical method that produces bilayers of aromatic DTs on gold by means of oxidative deposition [31], and Riskin et al. have reported the preparation with this procedure of 4,4′-biphenyl dithiol (BPhDT) monolayers on Au(111) to generate silver nanoclusters or functionalized electrodes [32].

The objective of this work has been to prepare and analyze layers of BPhDT molecules grown on Au(111) using different procedures. The layers were characterized with electrochemical reductive desorption, electrochemical impedance spectroscopy, blocking behavior of a redox couple, high-resolution X-ray photoemission spectroscopy (XPS), and surface-enhanced Raman spectroscopy (SERS). The aim has been to control the formation of S–S bonds, as one of the most important aspects to improve quality of the adlayers.

The different preparations involved the use of a polar and a non-polar solvent and a disulfide reducing agent (tris-carboxyethyl phosphine, TCEP). In the first part of our study we used electroreductive desorption to compare the outcomes of four preparation procedures; this analysis showed that the best results were obtained when the substrates were immersed in a solution of ethanol and TCEP. Then, in the second part of the study, the layers prepared in ethanolic solutions with and without TCEP were fully characterized using all the battery of techniques; this part of the study includes a series of SERS measurements performed in-situ during the growth of the layers.

2. Material and methods

2.1. Gold substrates

We used three types of Au substrates. A crystal, 4 mm in diameter, oriented better than 1° towards the (111)-face and polished down to 0.03 μm (MaTeck, Jülich, Germany) was used for all the electrochemical measurements; before the assembly process, the crystal was annealed in a hydrogen flame for 2 min, cooled under constant N_2 flux, and put in contact with water after 1 min. For the XPS measurements we used Au films evaporated on borosilicate glass (250 nm thick) provided by Arrandee; all the films were immersed in a hot piranha solution (H_2SO_4:H_2O_2, 70:30) during 30 s and then copiously washed with Milli-Q water, and before the assembly process they were annealed in a butane flame for 2 min and then cooled down to room temperature under constant N_2 flux. Finally, for the SERS measurements we used films with roughened surfaces prepared as follows: the films were electrochemically cleaned applying a voltage step of 2.4 V during 10 min in 0.5 M H_2SO_4 solution, then a linear potential sweep at 0.02 V s^{-1} from 2.4 to −0.6 V was applied [33], and finally they were rinsed with deionized water.

2.2. Preparation of SAMs

Biphenyl 4,4′-dithiol (abbreviated BPhDT) and tris-carboxyethyl phosphine (TCEP) were purchased from Sigma-Aldrich. Chemicals were used as received, without further purification. Pure ethanol and n-hexane (Baker) were used as solvents. The samples were immersed in 0.2 mM deoxygenated solutions at room temperature by different periods of time. The reducing agent was used in two ways, in post deposition treatments or added to the forming solution. In the post-deposition treatments freshly prepared BPhDT adlayers were introduced into a 4 mM aqueous solution of TCEP for 10 min (under sonication). In the other case, TCEP was first dissolved in Milli-Q water and then added to the forming solution; after that, the sample was washed in a TCEP concentrated solution. After the adlayers were formed the substrates were rinsed copiously with ethanol and Milli-Q water, blown dry with nitrogen, and quickly entered into the electrochemical cell (or vacuum chamber for the photoemission experiments). For more experimental details concerning sample preparation see Refs. [34,35].

2.3. Cyclic voltamperometry and impedance spectroscopy

Cyclic voltammograms (CV) and electrochemical impedance spectroscopy measurements were performed with a Solartron 1260 electrochemical interface and a conventional electrochemical three electrode cell with separate compartments for reference (Ag/AgCl (NaCl 3 M)) and a counter electrode (Pt wire). The electrolyte was thoroughly deaerated by bubbling with nitrogen prior to each experiment. CV experiments were performed in order to produce the reductive desorption as well as to evaluate the adlayers blocking behavior with a redox couple. Measurements were made at a sweep rate of 0.05 V/s. Electrochemical impedance spectra were recorded in the frequency range of 1 Hz–10 kHz. The signal amplitude to perturb the system was 0.01 V. All electrochemical measurements were performed at room temperature.

2.4. Photoelectron spectroscopy

The photoemission experiments were carried out at the D08A-SGM beamline of the Brazilian Synchrotron Light Laboratory (Campinas, Brazil). The pressure in the analyzer chamber was in the low 10^{-9} Torr range. Electron energy spectra were collected with a 150 mm hemispherical analyzer with its axis placed at 90° from the light beam and in the plane of the light polarization. The samples were mounted with the surface normal lying in the plane of the photon beam and electron emission directions, and at 45° from each direction.

The sample cleanliness was checked with survey spectra acquired with $h\nu = 600$ eV; only the characteristic peaks of Au, S and C were observed. Detailed S2p core-level spectra were measured at a photon energy of 300 eV. Before and after each spectrum we measured Au4f core-level spectra for count normalization and to calibrate the binding energies (BE) against that of the $Au4f_{7/2}$ core level at 84.0 eV. The S2p spectra were fitted with a linear background and three elemental components, each made of a pair of Voigt functions separated by 1.18 eV and fixed intensity ratio 2:1. The intensities, positions and Gaussian widths of the components were varied during the fittings; the Lorentzian width was kept fixed at 0.15 eV.

2.5. Surface-enhanced Raman spectroscopy

SERS experiments were performed on a Horiba LabRAM HR. The objective for laser illumination and signal collection was of a long working distance objective (8 mm) with a numerical aperture of 0.7 and a magnification of 100. The excitation line was from a 632.8 nm He–Ne laser, the power of the laser on the sample was about 5 mW.

3. Results and discussion

3.1. Electrochemical characterization

3.1.1. Reductive desorption

Electroreductive desorption in basic media is a valuable tool to analyze adlayers grown on metal substrates [36]. First, the potential at which the reductive desorption occurs depends on the adsorbate–substrate and adsorbate–adsorbate interactions, and thence it can be

used to identify the species being desorbed. Second, well-ordered adlayers produce narrow desorption peaks, and so the existence of disorder is often observed as a broadening of the peak. Finally, the area of the desorption peak is easily transformed into number of molecules desorbed per unit area, and hence it allows an accurate and absolute determination of the coverage. Therefore, in the first part of our study we used this technique to screen the results obtained with the different preparations. In Fig. 1 the CV profiles of the BPhDT layers grown on Au(111) substrates using different methods are presented and compared. The four preparations were: a) immersion 3 h in an ethanolic solution, b) immersion 1 h in a n-hexane solution in the absence of light, c) same as a) followed by a post-treatment with the disulfide reducing agent (TCEP), and d) same as a) but with the reducing agent added into the solution. The BPhDT concentration in all the solutions was 0.2 mM, and in c) the post treatment consisted in a further immersion of the modified substrate in 4 mM aqueous solution of TCEP for 10 min. In all cases the immersion bath and the electrochemical cell were interconnected and all the solutions were kept under a N_2 flux to prevent air oxidation.

The CV profile of the adlayer prepared by simple immersion in the ethanolic solution (Fig. 1a) presents two broad peaks centered at −918 and −1052 mV (fwhm ≈ 90 and 130 mV, respectively), and the charge in the two peaks amounts to Q = 163 μC/cm^2.

To interpret the CV profiles shown in Fig. 1 we recall briefly the reductive desorption of alkane and aromatic monothiols. In both cases the desorption occurs via the following reaction: [37].

$$RS-Au + e^- \rightarrow RS^- + Au \quad (1)$$

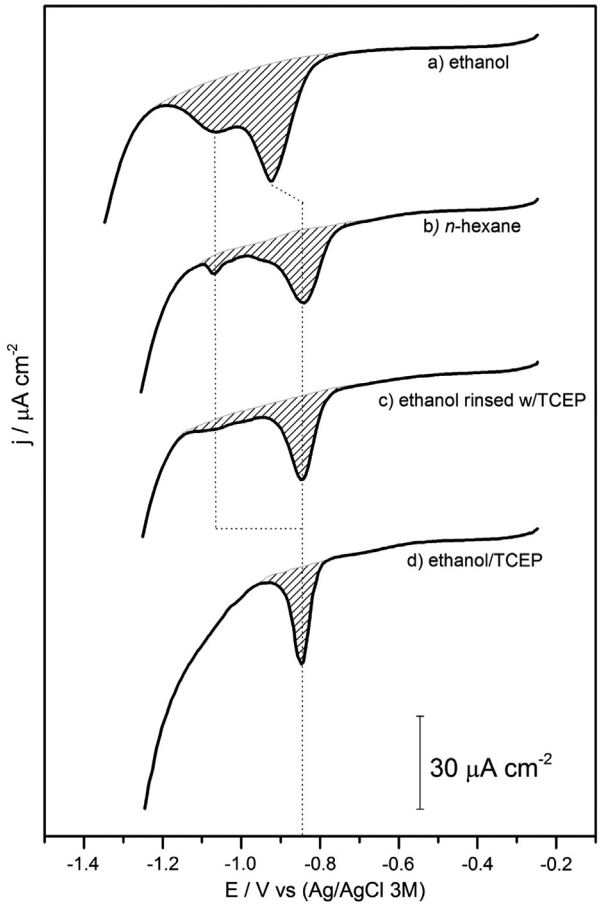

Fig. 1. Cyclic voltammograms recorded in 0.1 M KOH showing the reductive desorption profiles of BPhDT adlayers grown on Au(111) by four different methods. The areas used to calculate the desorption charges are shown in gray.

The CV profiles of the SAMs made of alkanethiols exhibit typically one narrow peak at a potential that becomes more negative as the number of C atoms in the chain increases [38]. For well-ordered SAMs the total integrated charge is always approximately the same: Q ≈ 75 μC/cm^2 (independent on the chain length), which according to Eq. (1) corresponds to a coverage θ ≈ 1/3 [39]. In the case of SAMs made of aromatic thiols the integrated charge is generally smaller, falling in the range 45–55 μC/cm^2; this implies a less dense layer [40–45], what is ascribed to the bigger size of the molecules. For example, Matei et al. [46] have found that SAMs made of 1,1′-biphenyl-4-thiol form a (2 × 2) structure instead of the (√3 × √3) structure typical of alkanethiols, which according to Eq. (1) yields Q = 56 μC/cm^2.

The reductive desorption of SAMs made of dithiols is more complex than those of monothiols because of the eventual presence of S–S bonds, which may become reduced in the cathodic sweep implying that two additional electrons are involved per S–S bond [6,7,35]. *Intralayer* (formed between neighboring DTs) and *interlayer* (formed from the terminal free –SH groups of the monolayer directly attached to the metallic substrate and those of DTs in solution) S–S bonds were detected in adlayers of DTs in a standing-up configuration [6,47,48]. Thus, in the reductive desorption of DT adlayers in alkaline media, in addition to Eq. 1 (with R = $^-$SRS − SRS), the following reactions should also be considered: [22].

a) Reductive desorption of a bi-layer of DTs, that occurs without the reduction of their *interlayer* S–S bond,

$$^-SRS–SRS–Au + e^- \rightarrow {}^-SRS–SRS^- + Au. \quad (2)$$

b) Reductive desorption when the S–S bonds of the DT dimers and DT-substrate bonds are reduced [49],

$$^-SRS–SRS–Au + 3e^- \rightarrow 2^-SRS^- + Au. \quad (3)$$

c) Reductive desorption of an adlayer containing *intralayer* S–S bonds (between neighboring DTs),

$$Au–SRS–SRS–Au + 4e^- \rightarrow 2^-SRS^- + 2Au. \quad (4)$$

Therefore, the very large charge in the CV profile of Fig. 1a indicates that the adlayer grown in the ethanolic solution must have a large amount of S–S bonds. If one assumes the existence of a single layer at a typical coverage for aromatic molecules, for example 0.22 ML which yields Q_{S-Au} ≈ 50 μC/cm^2, even assuming that all the molecules are dimerized in *intralayer* S–S bonds and that all the bonds become reduced in the cathodic sweep (Eq. 4) the integrated charge would be $Q_{S-Au} + Q_{S-S}$ ≈ 100 μC/cm^2, which is considerably smaller than the measured charge (163 μC/cm^2). Therefore, one must conclude that the preparation by immersion in the ethanolic solution results in at least a bilayer with a large amount of S–S bonds that become reduced mainly according to Eqs. (2) and (3).

The CV profile of the substrate immersed in the n-hexane solution (Fig. 1b) shows that the use of a non-polar solvent helps to improve the quality of the SAM [20–22]. The double peak has almost disappeared, and only a very small feature at −1068 mV remains; the main peak has shifted to a less negative potential (−847 mV), is narrower (fwhm ≈ 66 mV), and more importantly, the total charge has decreased to 80 μC/cm^2, denoting a large reduction of the number of S–S bonds. The CV profile in Fig. 1c shows that a similar result is obtained if after the immersion in the ethanolic solution the sample is rinsed with TCEP. The CV profile of this sample is composed of only one peak at −848 mV (fwhm ≈ 64 mV), with an integrated charge Q = 63 μC/cm^2, which denotes a further reduction of the number of S–S bonds. Finally, the CV profile in Fig. 1d shows that a further improvement is obtained if the reducing agent is added into the solution.

In this voltammogram there is again a single peak at −847 mV, but it is considerably narrower (fwhm 40 mV), and the integrated charge is also smaller: Q = 47.5 μC/cm^2. Since this charge is similar to that found in the desorption of aromatic monothiols we conclude that this preparation method resulted in the adlayer closest to the goal of a single layer free of S–S bonds.

Summarizing, the main results of the electroreductive desorption experiments are: i) despite the careful handling under a N_2 atmosphere to avoid the oxidative formation of S–S bonds, the immersion in pure ethanolic solutions results in adlayers with a large number of these bonds; ii) the use of a non-polar solvent like n-hexane in dark conditions reduced drastically the formation of these undesired bonds; iii) a similar result was obtained washing the substrate just immersed in the ethanolic solution with the reducing agent; and iv) the best result was obtained when the reducing agent was added to the forming solution; in this case both the fwhm and the charge of the current peak were similar to what is found in the desorption of SAMs made of aromatic monothiols.

In the next sections we present a more detailed analysis of the layers prepared with method d), aiming to demonstrate that these layers are composed of only one layer and are free of S–S bonds. To this purpose we performed additional electrochemical, photoemission and Raman measurements which are presented accompanied with the results obtained in substrates prepared by method a) for comparison.

3.1.2. Impedance spectroscopy

Fig. 2 presents Bode plots measured on substrates prepared by immersion in ethanolic solutions with and without TCEP. The results for a clean Au(111) substrate are also included for comparison. All the measurements were recorded at a potential of −300 mV, which is slightly more negative than the open circuit potential and more positive than the desorption potentials. The phase angle close to 90° and the log|Z| vs log(f) linear relationship observed at frequencies below 10 kHz are typical of a capacitive behavior. Accordingly, the curves were fitted with a $R_s(R_mCPE_m)$ circuit, where a constant phase element (CPE_m) accounts for the adlayer capacitance (C_m), which is in parallel with the adlayer resistance R_m, and R_s is the solution resistance. The fittings gave C_m = 24.0 μF/cm^2 for the clean Au(111) substrate and 6.0, and 3.3 μF/cm^2 for substrates with the adlayers grown in the solutions with and without TCEP, respectively. Furthermore, frequency dispersion CPE exponent α obtained for the fitting procedure was in the range $0.95 \leq \alpha \leq 1$, which can be attributed to highly packed SAMs. Since for a parallel plate capacitor C varies inversely with the thickness of the dielectric, the above results imply that the adlayer grown with TCEP in the forming solution is thinner than that prepared by immersion in the pure solution, what coincides with the conclusion reached above, that these preparations would lead to the formation of a monolayer and multilayers, respectively.

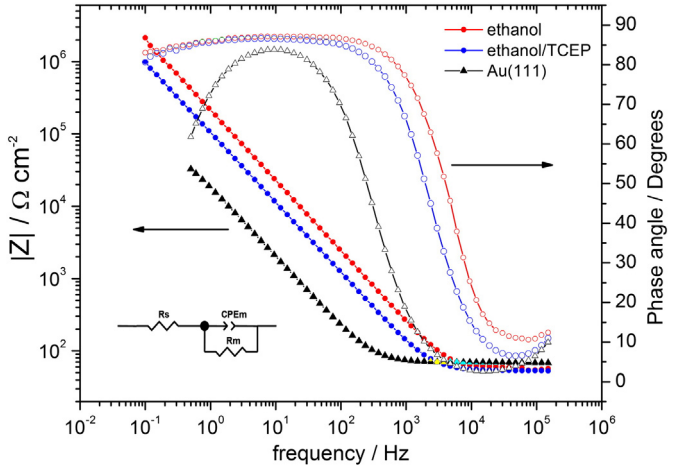

Fig. 2. Impedance modulus and phase angle vs. frequency measurements recorded in 0.1 M KOH of a clean Au(111) substrate (black) and substrates modified by BPhDT adlayers prepared by immersion 3 h in ethanolic solutions with (blue) and without (red) TCEP. The curves were fitted with the circuit shown in the inset. (For interpretation of the references to color in this figure legend, the reader is referred to the web version of this article.)

3.1.3. Blocking behavior of a redox couple

It is known that redox reactions occurring at the double layer in the electrode/solution interface can be blocked by the presence of a SAM on the electrode surface. This occurs because the electron-transfer rate between the metal electrode and the electroactive species in the solution is a function of the distance between them, in addition to other parameters as given by the Marcus theory [50]. Therefore, the same two adlayers probed above with impedance spectroscopy were also characterized by the CV response of the redox couple $K_4Fe(CN)_6/K_3Fe(CN)_6$. The results are presented in Fig. 3. Taking as reference the case of the clean Au(111) electrode, it is seen that the adlayer grown in the solution with TCEP (black line) reduces the redox activity more than 50%, while with the adlayer grown in the pure solution (dark-gray line) the activity is almost completely suppressed. This result implies again that the adlayer prepared with TCEP in the solution is thinner than the one prepared in the pure solution.

3.2. High-resolution photoemission spectroscopy

Fig. 4 presents the S2p core-level photoemission spectra of the adlayers grown in the solutions with and without TCEP. The S2p spectra of the SAMs made of dithiols are generally composed of two $2p_{1/2,3/2}$ doublets, one with the $2p_{3/2}$ peak located near 162 eV and another with this peak located near 163.3 eV [22,34,28–30,51]. The first doublet, which also appears in the spectra of SAMs made of monothiols, is ascribed to the S atoms bound to Au surface atoms, and the second to the S atoms in either S–H or S–S bonds. This large chemical shift between the two components facilitates the separate analysis of the S atoms at the Au/SAM interface and the other S atoms located at the SAM/vacuum interface and inside the SAM if there are multilayers. In particular, the two stable adsorption configurations of the molecules, LD or SU, have well-differentiated spectra. If the molecules are adsorbed LD on the surface only the first component at 162 eV should be observed, whereas if they are adsorbed SU both components should be observed with the component at 162 eV less intense than the other because of the electron attenuation inside the SAM. Since the two components at 162 and 163.3 eV are easily recognizable in the spectra of Fig. 4, it is immediately concluded that the molecules are adsorbed in

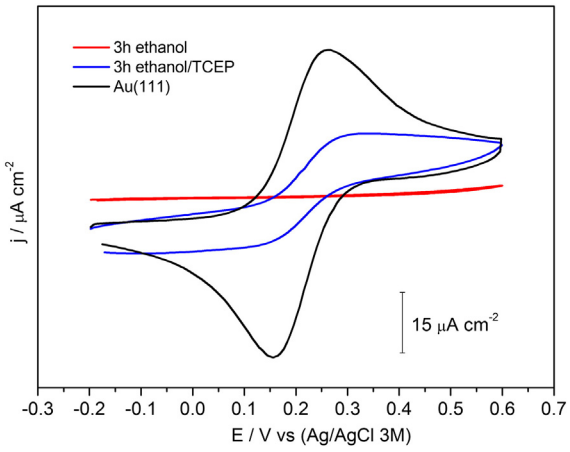

Fig. 3. Cyclic voltammograms for a $[Fe(CN)_6]^{4-}/[Fe(CN)_6]^{3-}$ couple onto a clean Au(111) substrate (black) and substrates modified by BPhDT adlayers prepared by immersion 3 h in ethanolic solutions with (blue) and without (red) TCEP. (For interpretation of the references to color in this figure legend, the reader is referred to the web version of this article.)

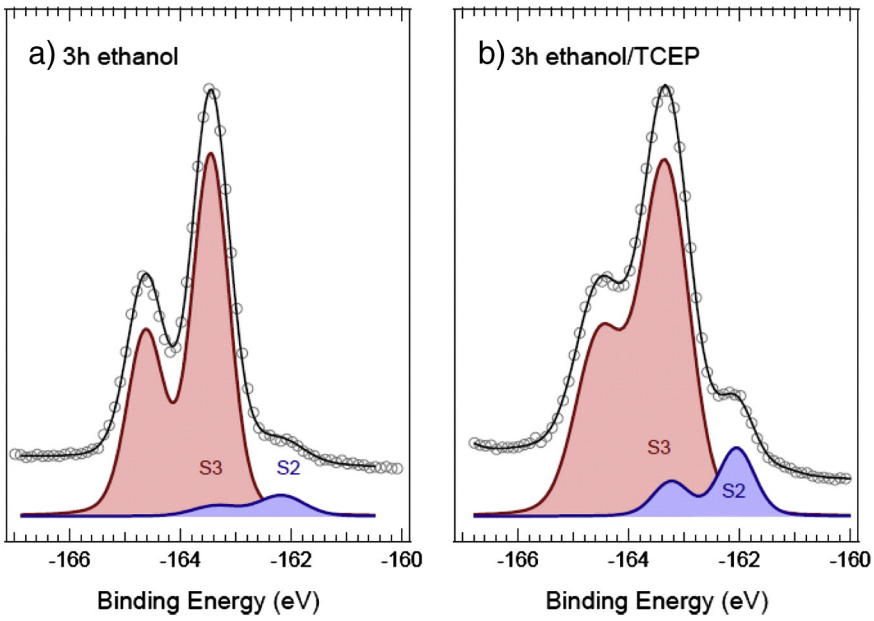

Fig. 4. S 2p photoemission spectra of Au(111) substrates with BPhDT adlayers prepared by immersion 3 h in: a) ethanolic solution, and b) ethanolic solution with TCEP.

the SU configuration in both preparations. This finding of a SU phase even when TCEP is added to the solution is in striking difference with the behavior of aliphatic dithiols, in which case it was found that the presence of the reducing agent in the forming solution prevents the lifting of the molecules [34]. It is also observed in Fig. 4 that the relative intensity of the component at 162 eV in the spectrum of panel b) is larger than in the spectrum of panel a); this difference implies that the layer grown with TCEP in the solution is thinner than the layer grown in the pure solution, in full agreement with the conclusions reached above with the electrochemical experiments.

Besides the qualitative analysis of the spectra, a quantitative comparison of the intensities allows the thickness and the surface coverage to be determined. To this purpose we fitted the spectra with three 2p-doublets, two to represent the components mentioned above and a third one, located near 161 eV, to account for the eventual presence of chemisorbed S atoms. The three doublets have been labeled S1–S3 in order of increasing binding energy (BE), and the two most important, S2 and S3, are shown in the figure together with the best fitting curves; all the fitting parameters are listed in Table 1.

We analyze first the case of a monolayer, which is simpler because the number of S atoms contributing to the components S2 and S3 (bottom and top layers, respectively) is the same; in this case the intensity ratio is well approximated by $S2/S3 = \exp(-t / \lambda \cos 45°)$, where t is the thickness of the layer, λ the attenuation length of the photoelectrons, and the cosine factor in the denominator appears because the emission is at 45° from the surface normal. Then, using $\lambda \approx 7$ Å [52] the ratio in the spectrum in Fig. 4b (S2/S3 = 0.15) is reproduced with $t = 9.4$ Å, which fits quite well with the expected thickness of a monolayer of BPhDT molecules adsorbed SU with the axis slightly tilted with respect to the surface normal ($d_{S-S} \approx 10.6$ Å in BPhDT). In the case of a bilayer one must expect a decrease of S2 because of the longer electron path inside the SAM, and an increase of S3 because of the contribution of the S atoms at the link between the two layers; the result is that the ratio S2/S3 for a bilayer should be smaller than the square of the ratio for the monolayer. Since S2/S3 in the spectrum of Fig. 4a is smaller than that of Fig. 4b but bigger than its square, we conclude that the thickness of this adlayer is intermediate between one and two layers. Therefore, these thicknesses derived from the spectra of Fig. 4 are also in agreement with the conclusions drawn in the analysis of the electrochemical experiments.

An estimate of the surface coverage can be obtained from the relative intensities of S2 and the Au4f peak, which represent the emissions from the bottom S-layer and the substrate, respectively. In this case, however, one must take into account the different photoemission cross-sections [53], the different attenuations of the S2p and Au4f photoelectrons inside the SAM [52], and also the attenuation of the latter inside the substrate [54]. Using cross-sections [53] and attenuation lengths taken from the literature [52,54] and assuming that the spectrum in Fig. 4b corresponds to a single layer, one finds that the ratio S2/Au4f = 0.084 corresponds to a coverage $\theta = 0.19$, which is in excellent agreement with the coverage determined with the area of the desorption peak in the CV profile of Fig. 1d.

Therefore, the analysis of the photoemission spectra of the substrates prepared in ethanolic solutions with and without TCEP confirms all the conclusions reached with the electrochemical experiments, namely the formation of a single layer in the first case and multilayers in the second case.

Table 1
Binding energy, Gaussian width, and relative area of the three components in the S2p photoemission spectra of Fig. 7.

	BPhDT 3 h ethanol			BPhDT 3 h ethanol/TCEP		
	S1	S2	S3	S1	S2	S3
BE (eV)	−160.85	−162.15	−163.40	−161.15	−162.05	−163.35
GW (eV)	0.6	0.9	0.7	0.6	0.7	0.9
Area (%)	0	6.6	93.4	0.8	12.9	86.3

3.3. Growth dynamics

In the previous sections we have shown with electrochemical and photoemission experiments that the simple immersion in an ethanolic solution leads to the formation of multilayers, and that the addition of TCEP into the solution limits the growth to only one layer. In this section, the dynamics of the self assembly process was monitored in-situ by means of surface-enhanced Raman spectroscopy. An important difference with the other experiments is that in this study the layers were not grown on flat Au(111) substrates, but on rough substrates (black gold) to exploit the surface-enhancement effect.

Fig. 5 presents the series of SERS spectra collected during the growth of the layers on substrates immersed in solutions with and without TCEP. The spectra were acquired in-situ as a function of the time elapsed

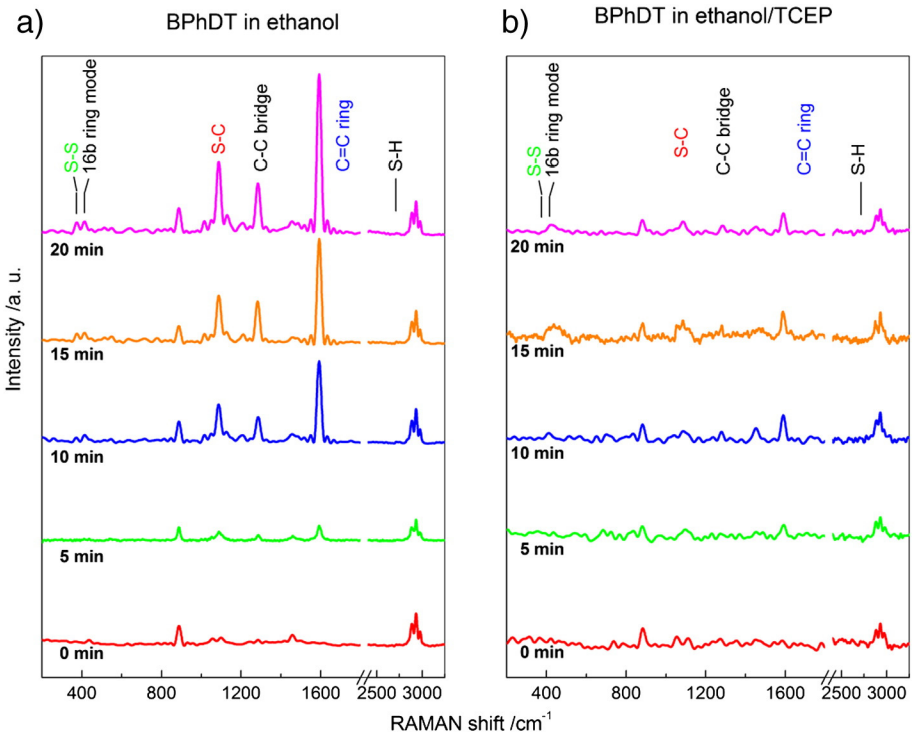

Fig. 5. SERS spectra acquired in situ with substrates immersed in: a) an ethanolic solution of BPhDT, and b) same with TCEP added to the solution. The spectra were recorded as a function of the time elapsed after the injection of the BPhDT molecules into the solutions. For convenience, the spectra were normalized to the intensity of the ethanol C – H stretching signals obtained at 2800–3010 cm^{-1}.

after the injection of the BPhDT molecules into the solutions. The two spectra at time zero were collected immediately before the injection of BPhDT molecules; therefore, these spectra contain the characteristic bands of ethanol: C – C stretching at 889.5 cm^{-1}, C – O stretching at 1059.1 cm^{-1}, $-CH_3$ rocking at 1102.7 cm^{-1}, $-CH_3$ bending at 1461.4 cm^{-1}, and C – H stretching at 2888.6, 2933, and 2978.9 cm^{-1} [55]. No signal corresponding to TCEP was detected in Fig. 5b. After the injection of the BPhDT molecules new signals appear that are identified as follows: S – S at 374.6 cm^{-1}, phenyl mode 16a at 409.3 cm^{-1}, S – C stretching at 1098 cm^{-1}, C – C stretching between the two phenyl rings at 1284 cm^{-1}, and C═C ring stretching at 1596 cm^{-1} [8,55–57]. The S – H stretching band at 2560 cm^{-1}, which was visible as a weak

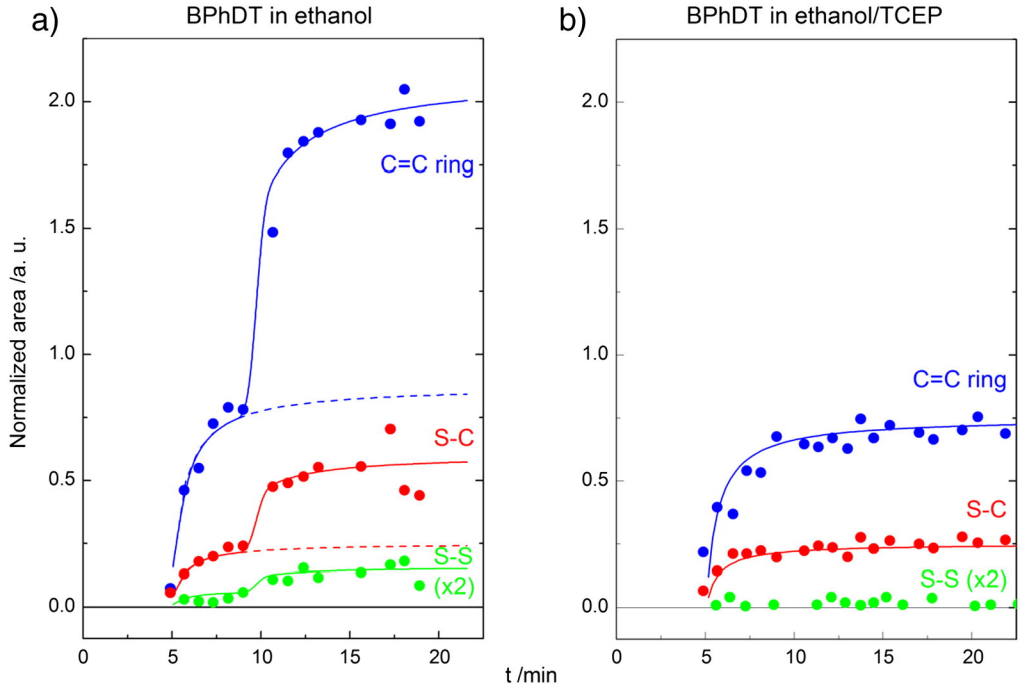

Fig. 6. Normalized area for the C═C ring, S – C, and S – S bands (at 1589, 1284, 375 cm^{-1}, respectively) in the spectra of Fig. 5 plotted as a function of time.

signal in reference spectra measured with solid BPhDT, is not detected in any of the spectra of the films, presumably because these bonds are too distant from the surface and thus there is no enhancement of the Raman signal. The increase with time of the BPhDT characteristic bands denotes the progress of the adsorption in both series. There are, however, two important differences that are worth to be noted. First, it is seen that the S – S band appears only in the spectra of the pure ethanolic solution, being absent in the spectra of the solution with TCEP. The second difference is related to the mode in which the BPhDT bands increase: while in the series of panel a) the intensities increase continuously, and in the series of panel b) the increase saturates at around 10 min. This difference is seen more clearly in the plots of the intensities as a function of time presented in Fig. 6. The first thing to be noted in this figure is that in both cases the increase of the signals is almost negligible during the first 5 min. After these initial minutes the intensities begin to increase and in the case of the solution with TCEP (Fig. 6b) they reach a plateau at about 10 min. Interestingly, in the case of the solution without TCEP (Fig. 6a) a new increase of the intensities begin to occur after 10 min, reaching a second plateau at around 15 min. These observations strongly suggest that the immersions produce the growths of a single layer in the case of the solution with TCEP, and a multilayer in the case of the solution without TCEP.

The evolution of the S – S signal at 374.5 cm^{-1} [8,55] is of particular interest. It can be seen in Fig. 6a that the intensity of this band does not rise up at 5 min like the other bands, but remains with a very low intensity (essentially within the detection limit) until about 10 min where it starts to increase. This indicates clearly that the S – S bonds begin to form only after completion of the first layer, and so one must conclude that intralayer S – S bonds are not formed in this system. This absence of S – S bonds between BPhDT molecules of the same layer (intralayer) is probably due to steric effects that impede the connection of their terminal groups. Turning to the layer grown in the solution with TCEP, it can be seen in Fig. 6b that the intensity of the S – S band remains within the detection limit at all times, a behavior that is consistent with the above finding that S – S bonds do not form in a single layer.

Therefore, although SERS cannot be used to test the layers grown on flat substrates, the results obtained in rough substrates confirm (and complete) the scenario depicted with the electrochemical and photoemission experiments, namely that the immersion in a pure ethanol solution produces multilayers, with the needed presence of (interlayer only) S – S bonds, whereas the immersion in a solution with TCEP produces the desired result of a monolayer free of any type of S – S bonds.

4. Conclusions

We have studied the formation of 4,4′-biphenyldithiol (BPhDT) adlayers on Au(111) using various preparation methods in solution phase. The best results were obtained when a disulfide reducing agent (TCEP) was added to the forming ethanolic solution. The adlayers grown by this method were characterized with five independent techniques: electroreductive desorption, impedance spectroscopy, redox activity, photoemission spectroscopy, and surface-enhanced Raman spectroscopy. All these characterizations were coincident in that this method of preparation leads to the formation of a monolayer of standing-up molecules, with a surface coverage $\theta \approx 0.2$, completely free of S – S bonds. It was also found that the immersion in pure ethanolic solutions leads to the growth of multilayers, in which only interlayer S – S bonds were detected. The growth dynamics followed by surface-enhanced Raman spectroscopy also showed that multilayers were formed if TCEP is not present in the forming solution.

Acknowledgments

Financial support from the Brazilian Synchrotron Light Laboratory (LNLS), FONCyT (Grants PICT 2005-33432 and 2005-32893), CONICET (Grants PIP 5903 and 112 200801 00958), and SECYT-UNC is gratefully acknowledged. Authors are also members of CONICET, Argentina.

References

[1] A. Ulman, An Introduction to Ultrathin Organic Films: Langmuir–Blodgett to Self Assembly, Academic Press, New York, 1991.
[2] L.H. Dubois, R.G. Nuzzo, Annu. Rev. Phys. Chem. 43 (1992) 437.
[3] M.A. Reed, C. Zhou, C.J. Muller, T.P. Burgin, J.M. Tour, Science 278 (1997) 252.
[4] B.S.T. Kasibhatla, A.P. Labonte, F. Zahid, R.G. Reifenberger, S. Datta, C.P. Kubiak, J. Phys. Chem. B 107 (2003) 12378.
[5] J. Liang, L.G. Rosa, G. Scoles, J. Phys. Chem. C 111 (2007) 17275.
[6] M.J. Esplandiu, M.L. Carot, F.P. Cometto, V.A. Macagno, E.M. Patrito, Surf. Sci. 600 (2006) 155.
[7] M.L. Carot, M.J. Esplandiu, F.P. Cometto, E.M. Patrito, V.A. Macagno, J. Electroanal. Chem. 579 (2005) 13.
[8] S.W. Joo, S.W. Han, J. Kim, J. Colloid Interface Sci. 240 (2001) 391.
[9] H. Rieley, G.K. Kendall, F.W. Zemicael, T.L. Smith, S. Yang, Langmuir 14 (1998) 5147.
[10] S. Kohale, S.M. Molina, B.L. Weeks, R. Khare, L.J. Hope-Weeks, Langmuir 23 (2007) 1258.
[11] T.Y.B. Leung, M.C. Gerstenberg, D.J. Lavrich, G. Scoles, F. Schreiber, G.E. Poirier, Langmuir 16 (2000) 549.
[12] W. Haiss, R.J. Nichols, H. van Zalinge, S.J. Higgins, D. Bethell, D.J. Schiffrin, Phys. Chem. Chem. Phys. 6 (2004) 4330.
[13] L. Pasquali, F. Terzi, R. Seeber, B.P. Doyle, S. Nannarone, J. Chem. Phys. 128 (2008) 134711.
[14] B. de Boer, M.M. Frank, Y.J. Chabal, W. Jiang, E. Garfunkel, Z. Bao, Langmuir 20 (2004) 1539.
[15] Y. Sakotsubo, T. Ohgi, D. Fujita, Y. Ootuka, Phys. E. 29 (2005) 601.
[16] H. Noda, Y. Tai, A. Shaporenko, M. Grunze, M. Zharnikov, J. Phys. Chem. B 109 (2005) 22371.
[17] K. Schouteden, N. Vandamme, E. Janssens, P. Lievens, C. Van Haesendonck, Surf. Sci. 602 (2008) 552.
[18] X.D. Cui, A. Primak, X. Zarate, J. Tomfohr, O.F. Sankey, A.L. Moore, T.A. Moore, D. Gust, G. Harris, S.M. Lindsay, Science 294 (2001) 571.
[19] D. García Raya, R. Madueño, M. Blazquez, T. Pineda, Langmuir 26 (2010) 11790.
[20] H. Hamoudi, Z. Guo, M. Prato, C. Dablemont, W.Q. Zheng, B. Bourguignon, M. Canepa, V.A. Esaulov, Phys. Chem. Chem. Phys. 10 (2008) 6836.
[21] H. Hamoudi, C. Dablemont, V.A. Esaulov, Surf. Sci. 605 (2011) 116.
[22] M.A. Daza Millone, H. Hamoudi, L. Rodríguez, A. Rubert, G.A. Benítez, M.E. Vela, R.C. Salvarezza, J.E. Gayone, E.A. Sánchez, O. Grizzi, C. Dablemont, V.A. Esaulov, Langmuir 25 (2009) 12945.
[23] A.O. Lundgren, F. Björefors, L.G.M. Olofsson, H. Elwing, Nanoletters 8 (2008) 3989.
[24] L. Venkataraman, J.E. Klare, C. Nuckolls, M.S. Hybertsen, M.L. Steigerwald, Nature 442 (2006) 904.
[25] F. Pauly, J.K. Viljas, J.C. Cuevas, G. Schön, Phys. Rev. B 77 (2008) 155312.
[26] L. Pasquali, F. Terzi, C. Zanardi, R. Seeber, G. Paolicelli, N. Mahne, S. Nannarone, J. Phys. Condens. Matter 19 (2007) 305020.
[27] L.S. Alarcon, L. Chen, V.A. Esaulov, J.E. Gayone, E.A. Sánchez, O. Grizzi, J. Phys. Chem. C 114 (2010) 19993.
[28] L. Pasquali, F. Terzi, C. Zanardi, L. Pigani, R. Seeber, G. Paolicelli, S.M. Suturin, N. Mahne, S. Nannarone, Surf. Sci. 601 (2007) 1419.
[29] H. Hamoudi, M. Prato, C. Dablemont, O. Cavalleri, M. Canepa, V.A. Esaulov, Langmuir 26 (2010) 7242.
[30] L. Pasquali, F. Terzi, R. Seeber, S. Nannarone, D. Datta, C. Dablemont, H. Hamoudi, M. Canepa, V.A. Esaulov, Langmuir 27 (2011) 4713.
[31] S. Rifai, M. Laferrière, D. Qu, D.D.M. Wayner, C.P. Wilde, M. Morin, J. Electroanal. Chem. 531 (2002) 111.
[32] M. Riskin, B. Basnar, V.I. Chegel, E. Katz, I. Willner, F. Shi, X. Zhang, J. Am. Chem. Soc. 128 (2006) 1253.
[33] N.G. Tognalli, A. Fainstein, C. Vericat, M.E. Vela, R.C. Salvarezza, J. Phys. Chem. B 110 (2006) 354.
[34] F.P. Cometto, G. Ruano, H. Ascolani, G. Zampieri, Langmuir 25 (2013) 1400.
[35] F.P. Cometto, C.A. Calderón, E.M. Euti, D.K. Jacquelín, M.A. Pérez, E.M. Patrito, V.A. Macagno, J. Electroanal. Chem. 661 (2011) 90.
[36] T. Kakiuchi, H. Usui, D. Hobara, M. Yamamoto, Langmuir 18 (2002) 5231.
[37] M.M. Walczak, D.D. Popenoe, R.S. Deinhammer, B.D. Lamp, C. Chung, M. Porter, Langmuir 7 (1991) 2687.
[38] O. Azzaroni, M.E. Vela, H. Martin, A. Hernández Creus, G. Andreasen, R.C. Salvarezza, Langmuir 17 (2001) 6647.
[39] C.A. Widrig, C. Chung, M.D. Porter, J. Electroanal. Chem. 310 (1991) 335.
[40] C.-J. Zhong, M. Porter, J. Am. Chem. Soc. 116 (1994) 11616.
[41] Y. Sato, F. Mizutani, Phys. Chem. Chem. Phys. 6 (2004) 1328.
[42] L.-J. Wan, M. Terashima, H. Noda, M. Osawa, J. Phys. Chem. B 104 (2000) 3563.
[43] F. Cometto, E.M. Patrito, P. Paredes-Olivera, G. Zampieri, H. Ascolani, Langmuir 28 (2012) 13624.
[44] E.A. Ramírez, E. Cortés, A.A. Rubert, P. Carro, G. Benítez, M.E. Vela, R.C. Salvarezza, Langmuir 28 (2012) 6839.
[45] D.E. Pissinis, O.E. Linarez Pérez, F.P. Cometto, M. López Teijelo, J. Electroanal. Chem. 712 (2014) 167.
[46] D.G. Matei, H. Muzik, A. Gölzhäuser, A. Turchanin, Langmuir 28 (2012) 13905.
[47] V.C. Ferreira, F. Silva, L.M. Abrantes, Chem. Biochem. Eng. Q. 23 (2009) 99.
[48] P. Kohli, K.K. Taylor, J.J. Harris, J.B. Blanchard, J. Am. Chem. Soc. 120 (1998) 11962.
[49] R. Kizek, J. Vacek, L. Trnková, F. Jelen, Bioelectrochemistry 63 (2004) 19.
[50] R.A. Marcus, N. Sutin, Biochim. Biophys. Acta 811 (1985) 265.

[51] Y. Tai, A. Shaporenko, H.-T. Rong, M. Buck, W. Eck, M. Grunze, M.J. Zharnikov, Phys. Chem. B 108 (2004) 16806.
[52] C.L.A. Lamont, J. Wilkes, Langmuir 15 (1999) 2037.
[53] J.J. Yeh, I. Lindau, At. Data Nucl. Data Tables 32 (1985) 1.
[54] A. Jablonski, C.J. Powell, J. Alloys Compd. 362 (2004) 26.
[55] R.M. Silverstein, F.X. Webster, Spectrometric Identification of Organic Compounds, 6th Edition Wiley, New York, 1998.
[56] L. Cui, B. Liu, D. Vonlanthen, M. Mayor, Y. Fu, J.-.F. Li, T. Wandlowski, J. Am. Chem. Soc. 133 (2011) 7332.
[57] W. Azzam, B.I. Wehner, R.A. Fischer, A. Terfort, C. Wöll, Langmuir 18 (2002) 7766.